Albena Doicheva[1], Yoshiki Shu[2], Fumio Kusuhara[2], Hitoshi Shiohara[2]*

SEISMIC TESTS ON REINFORCED CONCRETE BEAM-COLUMN JOINT SUB-ASSEMBLAGES SUBJECT TO LATERAL AND LONG-TERM VERTICAL LOAD

SEIZMIČKA ISPITIVANJA OJAČANIH BETONSKIH PODSKLOPOVA VEZA GREDA-STUB POD DEJSTVOM BOČNOG I DUGOTRAJNOG VERTIKALNOG OPTEREĆENJA

Originalni naučni rad / Original scientific paper
UDK /UDC:

Rad primljen / Paper received: 29.03.2022

Adresa autora / Author's address:
[1)] University of Architecture, Civil Engineering and Geodesy, Department of Technical Mechanics, Sofia, Bulgaria
[*]email: doicheva_fhe@uacg.bg
[2)] Department of Architectural Engineering of the University of Tokyo, Tokyo, Japan

Keywords
- reinforced concrete
- beam-to-column joint
- long-term shear force
- column-to-beam strength ratio
- joint damage

Abstract

The testing of the one-third scale four plane reinforced concrete interior beam-column joint sub-assemblages are presented in this paper. The specimens are designed to allow for a beam yielding mechanism by limiting the joint shear and are statically cyclic loaded in both directions with increasing amplitude. Variables of the test are chosen as with or without a constant downward force simulating gravity load on the beams and the column-to-beam strength ratio. Severe beam-column joint damage is observed in some specimens. In specimens with column-to-beam strength ratio of 1.18, with simulated gravity load on the beams, yielding of the longitudinal reinforcement in top column occurred at an early stage and only the deflection of top columns progressed. This trend was not observed in other specimens without simulating gravity load or specimens with column-to-beam strength ratio of 2.22.

Ključne reči
- ojačani beton
- veza greda - stub
- dugotrajna sila smicanja
- odnos nosivosti stub-greda
- oštećenje veze

Izvod

U radu je predstavljeno ispitivanje četiri ravanski ojačanih betonskih unutrašnjih podsklopova veza greda-stub u trećini razmere. Uzorci su projektovani tako da se u njima javlja mehanizam tečenja grede ograničenim smicanjem u vezama, a takođe su statički ciklično opterećeni u oba pravca sa porastom amplitude. Parametri ispitivanja su izabrani sa ili bez postojanja konstantne vertikalne sile na dole, simulirajući gravitaciono opterećenje na grede i na odnos nosivosti stub-greda. Uočeno je znatno oštećenje veze greda-stub kod nekih uzoraka. Kod uzoraka sa odnosom nosivosti stub-greda od 1,18 sa simulacijom gravitacionog opterećenja na grede, u ranoj fazi se pojavljuje tečenje podužnog ojačanja u gornjem stubu, a samo se uvećavao ugib gornjih stubova. Ovaj trend nije uočen kod ostalih uzoraka bez simulacije gravitacije, ili kod uzoraka sa odnosom nosivosti stub-greda od 2,22.

INTRODUCTION

Dead and live loads act on building structures as a result of constant weight of the structure and the fixture of the building. They are transferred to the ground through the floor slabs and the beams to the columns via beam-column joints. Despite to the reality, in usual seismic test setups of reinforced concrete beam-column joint sub-assemblages, the constant vertical load is not loaded on the beams to simplify the loading condition. As a result, the effect of the constant vertical load on beams on the earthquake response of the moment resisting frames has not been fully identified and verified by experiments.

In large scale shaking table tests of the building structure, the effect of constant vertical load is inherently included. But it does not justify the ignorance of the effect of vertical load in the design where structural modelling of moment resisting frame structure is necessary. There has been little study which intends to investigate the effect experimentally and systematically by the cyclic static load method. Hence, static cyclic loading tests of reinforced concrete interior beam-column joint sub-assemblages were carried out. The effects of the presence or absence of long-term shear force in beams are investigated in the tests. The impact of the test results on the structural modelling and design issues are discussed in the paper.

PLAN OF TESTS

One of the reasons the authors pay special attention to the effect of constant vertical shear in a beam is the recently identified mechanism of joint hinging in reinforced concrete beam-column joint /1-3/. Joint hinging occurs to the beam-column joint with column-to-beam strength ratio (MR ratio) near 1.0. The joint hinging mechanism is defined by the tensile yielding of longitudinal bars passing through a beam-column joint in vertical and horizontal direction under lateral loading /1/. As a result, the damage of diagonal cracking and concrete crushing are concentrated at the connection of beams and columns. This joint hinging mechanism develops even if the beam-column joint satisfies the current seismic design provisions /4/ on joint shear force and the minimum joint shear reinforcement. In addition to that, the lateral

strength of the structural system is jeopardized due to joint hinging mechanism. It is reported that MR ratio needs to be larger than 1.5 for interior beam-column joints /2/, and 1.8 for exterior beam-column joints /3/, in order to obtain satisfactory lateral capacity of structural system compared to the calculated capacity of the beam by flexural theory.

Hence, reinforced concrete moment resisting structures conformed to current seismic provision are vulnerable to the joint hinging mechanism. It means, when damage to the beam-column joints occurs due to the joint hinging mechanism, the mechanism of long-term shear and moment transferred from the beams (hereinafter, referred to as 'long-term shear force') to the columns is something different from what engineers had thought before. So, an experiment plan is made to investigate two variables: (1) the presence or absence of a long-term shear force in the beam; and (2) the MR ratio.

Test parameters

Specimens were one-third scale beam-column joint subassemblages of a crucial form. The dimensions, reinforcement, and some parameters of the four exemplars are listed in Table 1, while Fig. 1 shows the geometry and dimensions of the specimens. The depth and width of all beams and columns is 240 mm. The main reinforcement is with SD345; for beams it is 5D13 bottom and top; 4D13 for columns of specimens I04 and I05, and 6D13 for specimens I06 and I07.

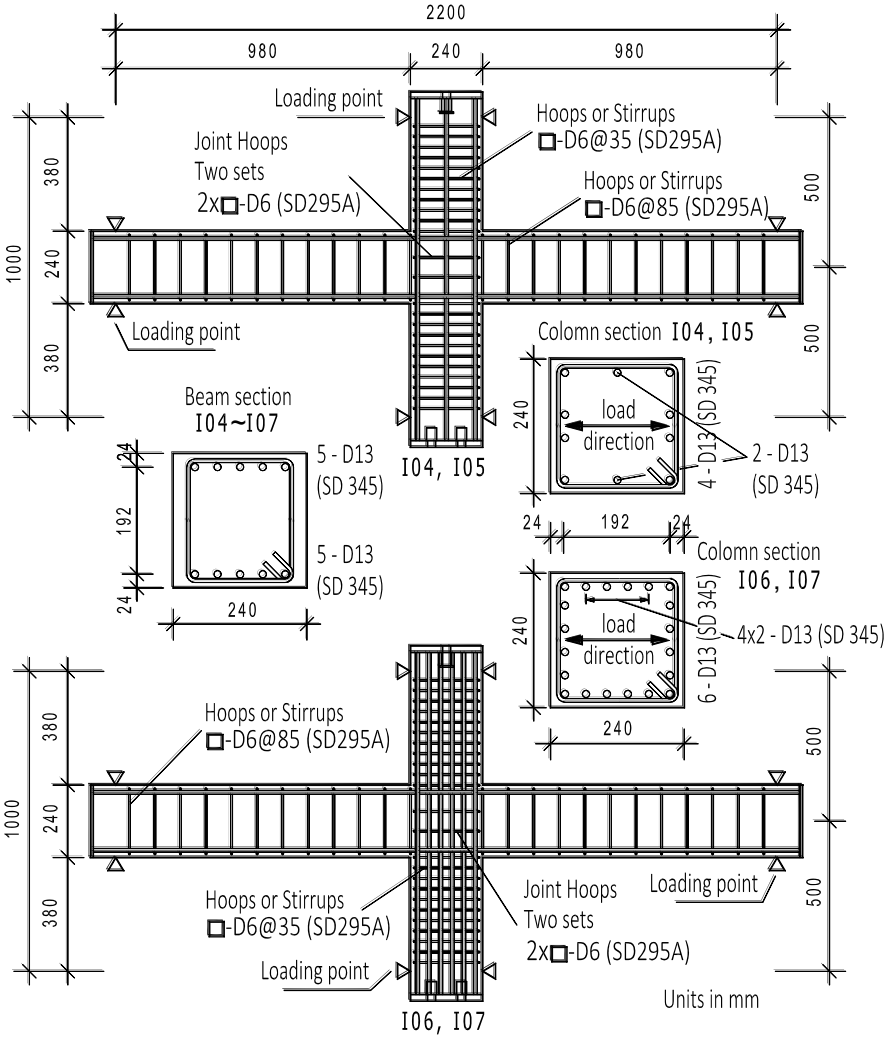

Figure 1. Dimensions and reinforcement of specimens.

A test of four specimens is planned. Specimens I04 and I05 are of identical reinforcement and shape, while long-term shear force of the beam is present (in I05), or absent (in I04). Specimens I06 and I07 are also of identical shape and differ only with regard to the presence or absence of a long-term shear force of the beam. Specimens I04 and I05, respectively I06 and I07, are with identical beams and reinforcement, but the column main reinforcement is increased in the second couple. The long-term load was applied on test specimens I05 and I07.

Cross-sectional analysis was accomplished by using the material test results and assuming plane behaviour. The beam-to-column intensity ratio was calculated based on the ultimate moment; it was 1.18 for specimens I04 and I05 and 2.22 for I06 and I07.

The hoops and stirrups of all the specimens are of rectangular shape of D6 (SD295A) deformed bars at different spacing in accordance with Fig. 1. Two sets of rectangular hoops of D6 deformed bars are provided in the horizontal direction in a joint of all the specimens /4/. The joint shear

reinforcement ratio is approximately 0.3 % and satisfies the minimum requirement of the AIJ Guidelines, /4/.

Table 1. Specifications of the specimens.

Specimens	I04 (I05)	I06 (I07)
span $L_b \times L_c$ [mm]	2200 × 1000	
beam and column cross-section b×D [mm]	240 × 240	
beams longitudinal reinforcing bar	5-D13 (SD345)	
beam tensile reinforcement ratio [%]	1.22	
beam stirrups	□-D6@85	
beam shear reinforcement ratio [%]	0.31	
column tensile main reinforcement	4-D13 (SD345)	6-D13 (SD345)
column tensile reinforcement ratio [%]	0.98	1.47
intermediate reinforcement	2-D13 (SD345)	4-D13 (SD345)
column stirrups	□ - D6@35	
column shear reinforcement ratio [%]	0.75	
joint hoops	□-D6(SD295)ps	
joint horizontal reinforcement ratio [%]	0.28	
column axis force	0	
joint shear margin*	1.73	
column-to-beam strength ratio (MR ratio)	1.18	2.22
bond capacity margin**	0.96	

* Joint shear margin: ratio of joint shear force to the joint shear capacity calculated by the AIJ Guidelines /4/.

** Bond capacity margin: ratio of bond stress of the longitudinal reinforcement passing through the joint to bond capacity calculated by the AIJ Guidelines /4/.

Material properties

High strength concrete was used with material properties as shown in Table 2. Concrete compressive strength was tested by a 100 by 200 mm cylinder. It was 51.6 MPa and the measured compressive strain was 2230×10^{-6}. During tensile tests the reinforcement bars demonstrated yield points of 375 and 334 MPa for D13 (SD345) and D6 (SD295), respectively. All results of the reinforcement tests are summarized in Table 3.

Table 2. Material properties of concrete.

	Compressive strength [MPa]	Compressive strain [$\times 10^{-6}$]	Young's modulus [GPa]	Splitting strength [MPa]
Concret	51.6	2230	33.1	3.82

Table 3. Material properties of reinforcing bars.

	Yield point [MPa]	Tensile strength [MPa]	Young's modulus [GPa]	Fracture strain [%]
D13 (SD345)	375	532	185	19.7
D6 (SD295)	334	479	186	23.6

Loading setups

Loading setups are shown in Fig. 2. The upper horizontal loading beam was supported by two vertical loading columns with pinned joints at both ends. Vertical loading columns were connected to a lower horizontal loading beam by a pinned joint. The lower loading beam was fixed to a testing floor. A specimen was connected by a set of horizontal and vertical PC rods to a loading steel frame. The distance between loading points at beam ends was 2200 mm and at the ends of columns 1000 mm. By applying a horizontal displacement to the upper loading column by an oil jack, a beam-column joint specimen was forced to deform like in a moment resisting frame. A long-term shear force was simulated by vertical PC rods tensioned by means of springs. The constant of the spring used was 75.89 N/mm.

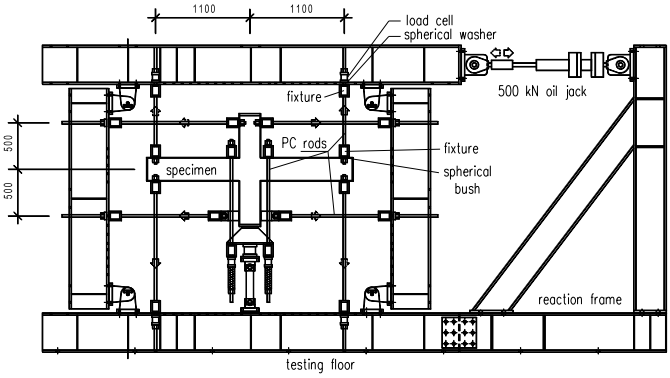

Figure 2. Force application equipment.

Loading cycles

Statically cyclic lateral load reversals with increasing amplitude were applied to the specimens to achieve a load-deformation relation. The first loading cycle was with load control to confirm the initial stiffness of specimen before cracking. The shear force was 11 kN; it was applied in the positive and negative alternating cyclic static load. One reversal cyclic load was applied with displacement control at each story drift ratio of 0.25 % and 0.5 %. Three reversal cycles followed at each story drift ratio of 1.0 %, 1.5 %, 2.0 %, 3.0 %, 4.0 % and 5.0 %. No axial force in columns and beams was applied during the test in specimens I04 and I06; in specimens I05 and I06 there was an axial force in the lower story of columns alone caused by a long-term shear force (Fig. 3). This force was calculated for an area of 8 m beam span and 6 m of the span transverse direction and for distributed load of the floor 10 kN/m^2. The calculated value of the long-term shear force was 240 kN. Because of the scale of test specimen (1/3), the long-term shear force for the experiment was scaled down to 1/3. The calculated experimental force was divided into two - 15kN and 12kN. The first was allowed to act at 75 mm from the beam face position and the second was applied at the beam tip (Fig. 3).

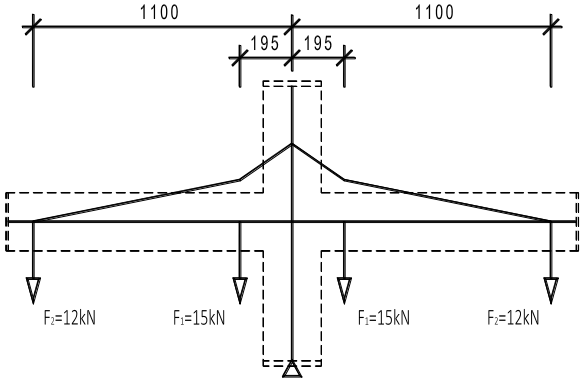

Figure 3. Distribution of long-term shear force.

Measurements

The shear story force was measured by reading the force with load cells that were installed at the end of vertical PC

rods. The story drift ratio was measured as the difference of the lateral displacement at the two inflection points in the column divided by the distance of the inflection points (= 1000 mm). The strain on the longitudinal reinforcing bars in beams and columns as well as in joints was measured by strain gauges. The cracks at the column face and in the joint were measured.

The long-term shear force at 75 mm from the beam face position varied with the deformation. Shearing force acted by deforming the spring. The rigidity of PC steel bars was high, and the deformation of the specimen affected the deformation of the spring, hence the size of the shear force. For I05, within 3 % story drift ratio the magnitude of the shear force varied within 5 % of 15 kN; with greater change as the story drift ratio increased, a change of up to about 16 % occurred. Within 3 % story drift ratio the shear force fluctuated within 5 % of 15 kN for I07, and the greater the change as the story drift angle increased, it varied up to about 11 %.

Because the shearing force of the beam tip varied with deformation, it was adjusted at the time of unloading of the loading cycle. It should be noted that this adjustment was after the unloading for the third time to the negative side and started after 2 % story drift ratio for I05, and from 0.5 % story drift ratio for I07. At the time of loading this shear force was derived by measuring the load cell from the tensile force in the vertical direction of PC steel bars and it was determined from the equilibrium of the moment around the joint.

TEST RESULTS

Overall behaviour

The damages in the story drift ratio of 2 % of the loading cycle of each specimen are shown in Fig. 4. For each of the test specimens, the first crack was a diagonal one at the corner. These cracks occurred in the corner of the joint between the beams and columns. They were followed by diagonal cracks at the centre of the joint. The deformation was concentrated at the joint. The diagonal cracks at the centre of the joint and diagonal cracks at the corner ex

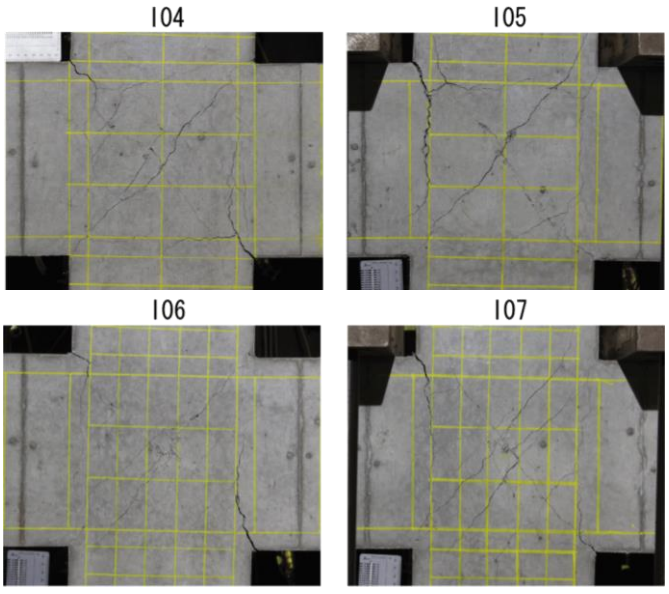

Figure 4. Typical damages of beam-column joints at story drift.

panded. At load cycles with story drift ratio of 2.0 %, concrete crushing at the centre of the joint started and cover concrete spalled off at the load cycle with story drift ratio of 3.0 % or more. When the story drift ratio of 5 % of the loading cycle was finished, the concrete of the joint surface was about half flaked off, part of the joint lateral reinforcement and column middle bars were visible. In the two specimens with long term shear force (I05 and I07) pairing of the diagonal cracks was observed; one of the pairs entered into the upper column side to less than 30 mm from the corner of the beam column rather than entering the corners of the beam-column joints. When comparing specimen I05 with I04 and specimen I07 with I06, the damage to the position close to the corner portion of the upper column was larger for specimens with long-term shear force (I05 and I07).

Table 4. Experimental results.

		I04	I05	I06	I07
Diagonal cracks at the corner	positive	18.4 0.06	- -	24.0 0.09	- -
	negative	-13.1 -0.02	- -	-21.6 -0.04	- -
Diagonal cracks at the centre of the joint	positive	70.4 0.67	72.1 0.66	27.7 0.13	47.1 0.32
	negative	-46.8 -0.35	-59.9 -0.56	-29.2 -0.12	-40.3 -0.21
Yielding of longitudinal bars in beams	positive	101 1.15	72.1 0.66	108 1.00	76.1 0.60
	negative	-97.7 -1.76	-72.1 -0.71	-101 -0.86	-83.7 -0.65
Yielding of longitudinal bars in columns	positive	101 1.15	85.5 1.10	no yielding	no yielding
	negative	-90.8 -1.16	-85.6 -0.96	-103 -2.11	-101 -3.60
Joint horizontal reinforcement yielding		101 1.15	-85.6 -0.96	97.0 0.83	-88.2 -0.70
Maximum story shear force	positive	115 2.95	112 4.01	116 1.50	121 2.97
	negative	-105 -3.01	-105 -2.91	-112 -3.00	-112 -2.82

top row shearing force [kN], lower row: story drift [%]

Yielding of reinforcement

A list of experimental results is shown in Table 4. In each test specimen the beam main reinforcement yielded at story drift of 0.6 to 1.2 %. When comparing specimens I05 and I07 with I04 and I06, respectively, the shear force at the moment of beam main reinforcement yielding was smaller for the first couple. It is because when there is a long-term shearing force at I05 and I07, the tensile forces in the longitudinal bars of the top of the beam increase and a compressive force to the main reinforcement of the beam bottom occurs. In I04 the column main reinforcement yielded almost simultaneously with the beam main reinforcement or a bit later during the same loading cycle. In I05 the beam top and the lower main reinforcement and upper column main reinforcement yielded before the bottom column main reinforcement. The column main reinforcement did not yield at the loading of the positive side for specimens I06 and I07 because column intensity ratio was large, but it yielded in the loading of the negative side at the time of the 2-3 % story drift ratio. Joint horizontal reinforcement yielded in

each specimen from 0.7 to 1.2 % story drift ratio. When the horizontal reinforcement yielded, the shear force in I05 was 15 % smaller than in I04, and in I07 it was 9.1 % smaller compared with the shear force in I06.

Story shear force-story drift ratio relation

The relation of story shear force to story drift ratio of each specimen is shown in Fig. 5; the story shear force calculated by the flexural theory of the section is shown there with horizontal dotted line. Two calculated values of story shear force are shown - with and without considering the strain hardening of the steel reinforcement. The calculated value with considered strain hardening of the steel reinforcement is based on the proposed solution of Park and Paulay /5/.

The hysteresis loop of all specimens demonstrated slip properties. The column strength ratio was greater for I06 and I07, and compared with I04 and I05, became bulging for a more hysteresis loop.

Specimen I04 reached maximum shear force of 114.8 kN for story drift ratio 3 % of the loading cycle. Specimen I05 reached the maximum shear force of 112.5 kN for story drift ratio 4 % of the force application cycle. Specimen I06 reached maximal shear force of 116.3 kN for story drift ratio 1.5 % of the force application cycle, and specimen I07 reached the maximal shear force of 120.9 kN for story drift ratio 3 % of the loading cycle. The measured value of the maximal shear force of all specimens was higher than the calculated value by flexural theory of the section without considering the strain hardening of steel reinforcement. The measured value of maximal shear force for specimens I04, I05 and I06 was lower than the calculated value of the shear force and considered strain hardening of steel reinforcement with 1.8 %, 3.8 %, and 0.5 %, respectively. The measured value of maximal shear force for specimen I07 exceeded the calculated value with considered strain hardening of steel reinforcement by 3.4 %. Analysis of data at the yielding of the beam main reinforcement at the maximum shear force of each test specimen shows that the strain exceeded the one obtained in the initial materials test and the influence of the strain hardening of steel reinforcement to the maximum strength of each test specimen, should also be considered.

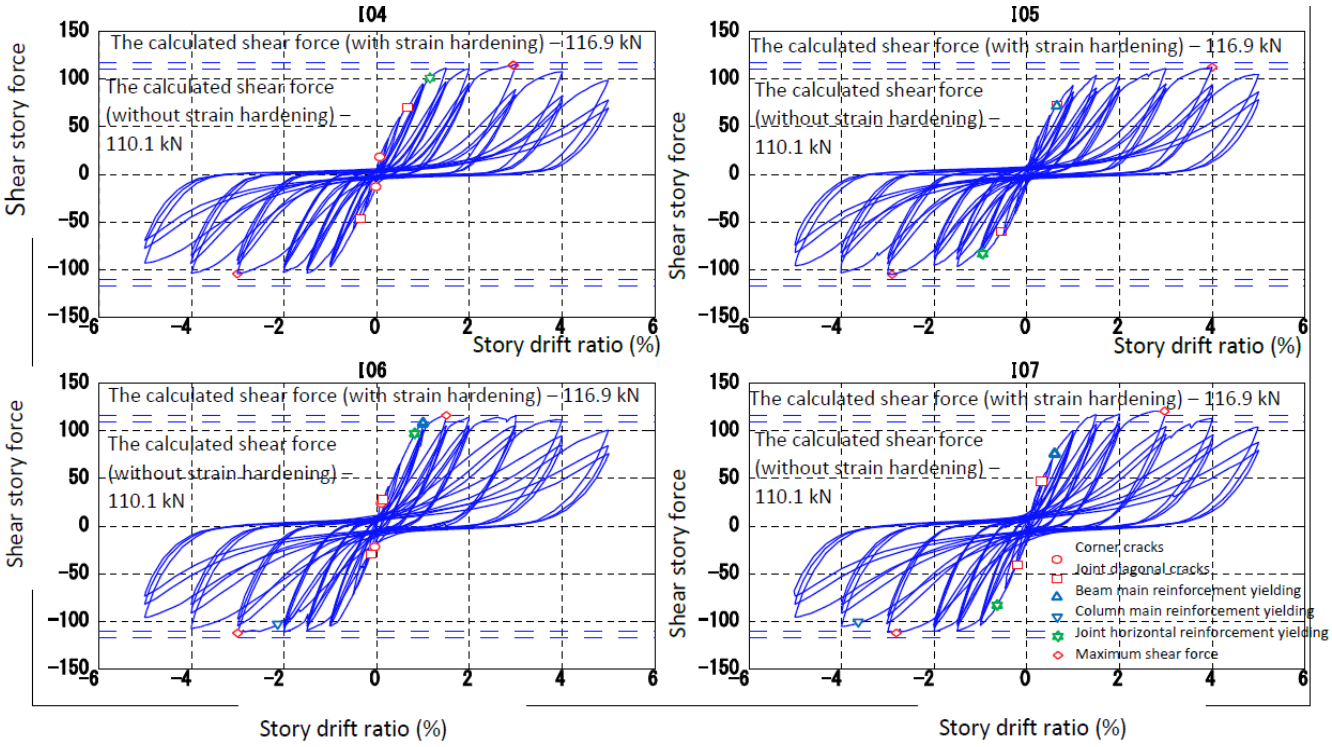

Figure 5. Story shear-story drift relations.

Rotation of the upper and lower column end

The relation of the story drift ratio and the node moment due to rotational component /6/ of the upper and lower column end to the story drift ratio 2 % of each specimen is shown in Fig. 6. Maximum rotations were measured at specimens with smaller beam-column intensity ratio. The rotation of the lower column end in I04 without long-term shear force was greater than that of the upper column end. For specimen I05 (with long term shear force) the upper column deformation was about 2.6 times greater than the deformation of the lower column. For specimens with long-term shear force, yielding of the upper column main reinforcement occurs in the early stages of loading and only the top posts were greatly deformed. On the other hand, in the specimens with large beam-column intensity ratio, the deformation of the under column for I06 without long-term shear force was slightly larger than the above posts. In I07 with long-term shear force, the rotation of the under column was the same as in I06 but a little larger than at the top posts.

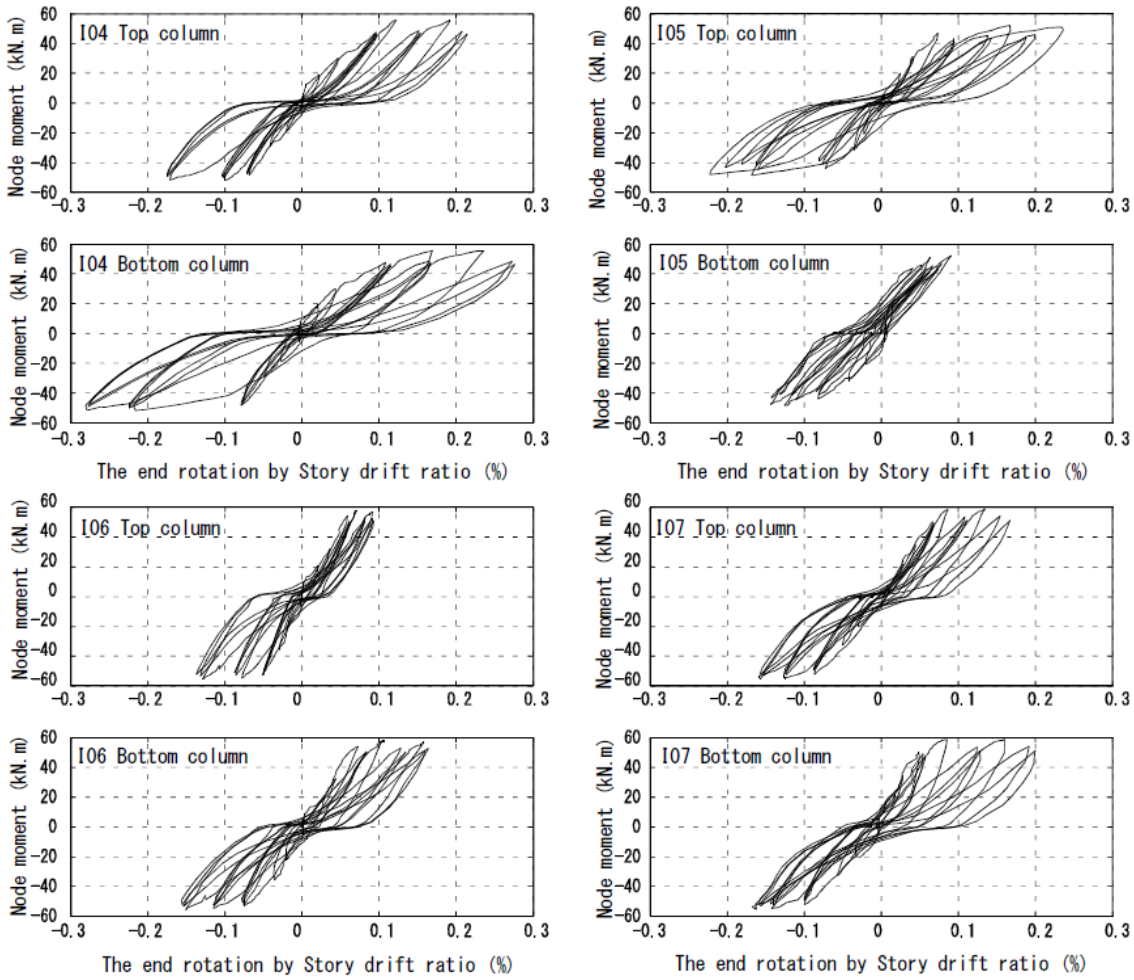

Figure 6. Rotation of the upper and lower column end.

Table 5. Stiffness of the experimental value.

		I04	I05	I06	I07
Initial stiffness		329	282	342	255
Beam main reinforcement yielding stiffness		88.0 (0.27)	111 (0.39)	108 (0.32)	136 (0.53)
Unloading stiffness (ratio to initial stiffness)	1.0%	150 (0.46)	135 (0.48)	166 (0.48)	167 (0.65)
	1.5%	130 (0.39)	128 (0.45)	147 (0.43)	154 (0.60)
	2.0%	122 (0.37)	122 (0.43)	134 (0.39)	145 (0.57)
	3.0%	116 (0.35)	116 (0.41)	125 (0.37)	126 (0.49)
	4.0%	107 (0.33)	113 (0.40)	122 (0.36)	121 (0.47)
	5.0%	100 (0.31)	116 (0.41)	112 (0.33)	117 (0.46)

DISCUSSION

Stiffness and restoring force characteristics

Three modules for secant stiffness obtained from the relation of the shear force and the story drift ratio are shown in Table 5. The initial stiffness of the shear force is the secant stiffness connecting the positive and negative peak of force application cycle that occurs at 11 kN. Beam main reinforcement yielding stiffness is secant stiffness of the first yielding of the beam main reinforcement. Unloading stiffness is defined as the average of the secant stiffness connecting points from 1/3 unloaded pressure forces of the second peak and the third peak of the loading cycle.

Initial stiffness of I05 was 85.8 % of I04 and initial stiffness of I07 was 74.5 % of I06. In I05 and I07, long-term shear force and moment were input to the junction before the horizontal force application, since diagonal cracks in the corner portion occurred, the initial stiffness of the I05 and I07 was smaller than the respective one in I04 and I06.

Specimens with long-term shear force had higher beam main reinforcement yielding stiffness than the specimens where long-term shear force was absent. In I05 and I07 the beam main reinforcement yielding stiffness was 126 % more than I04 and I06, respectively.

In all the specimens (I04, I05, I06 and I07) the unloading stiffness decreases with the increase of the story drift ratio. Specimens with large column intensity ratio, I06 and I07, were with higher unloading stiffness as compared to specimens I04 and I05.

The decrease in strength due to the increase of deformation

The rate of decrease in strength for the first time of the peak value of the positive and negative side of each loading cycle after maximum strength to the maximum story drift ratio of each specimen is shown in Fig. 7.

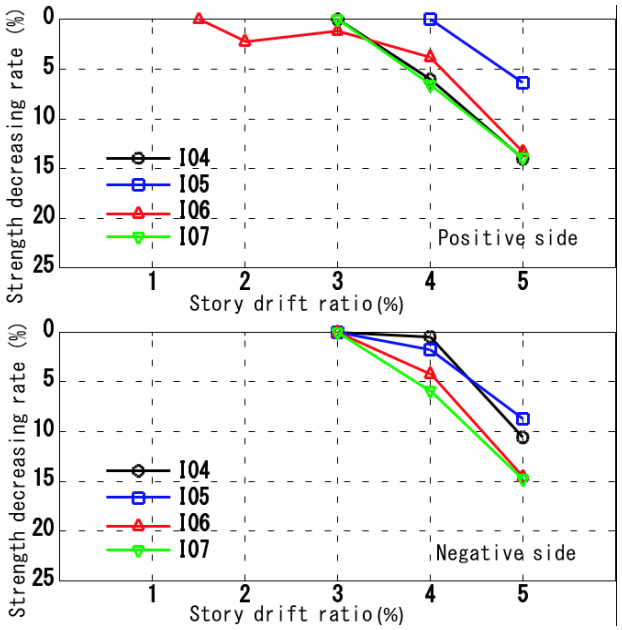

Figure 7. Proportion of strength reduction due to cyclic loading.

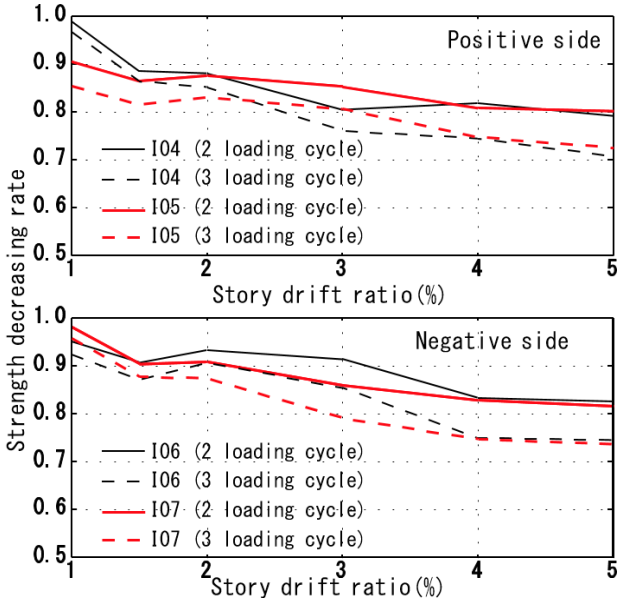

Figure 8. Proportion of strength reduction due to loading cycle.

For all test specimens with the increase of deformation angle the shear force of the first loading cycle was decreasing. The maximum strength of each test specimen in the positive side was different for all story drift ratios. In the negative side of each test specimen the maximum strength occurred at story drift ratio 3 %. Strength decreases with high rate with the increase of beam-column strength ratio and no considerable difference was observed in I06 and I07.

The decrease in strength due to cyclic loading

The decreasing ratio between average values of shear strength on the second and the third of the positive and negative peaks of the loading and the shear strength of the forces from the positive-side peak of the first loading cycle of each specimen is shown in Fig. 8.

In all specimens, as the story drift ratio increases, the strength reduction rate due to the first loading cycle decreased. For I04, I05, I06, I07 the ratio of shear strength on the second loading cycle to the shear strength of the forces from the positive-side peak of the first loading cycle was respectively up to about 21 %, 20 %, 17 %, and 18 %. The decreasing ratio was obvious in the third loading cycle, and it was reduced with 27 %, 29 %, 25 %, 24 %, respectively with regard to the first loading cycle.

Hysteresis absorbed energy - equivalent viscous damping constant

The hysteresis absorbed energy (the area of one cycle to hysteresis loop from shear force and displacement) of one cycle of each specimen is shown in Fig. 9 - equivalent viscous damping constant.

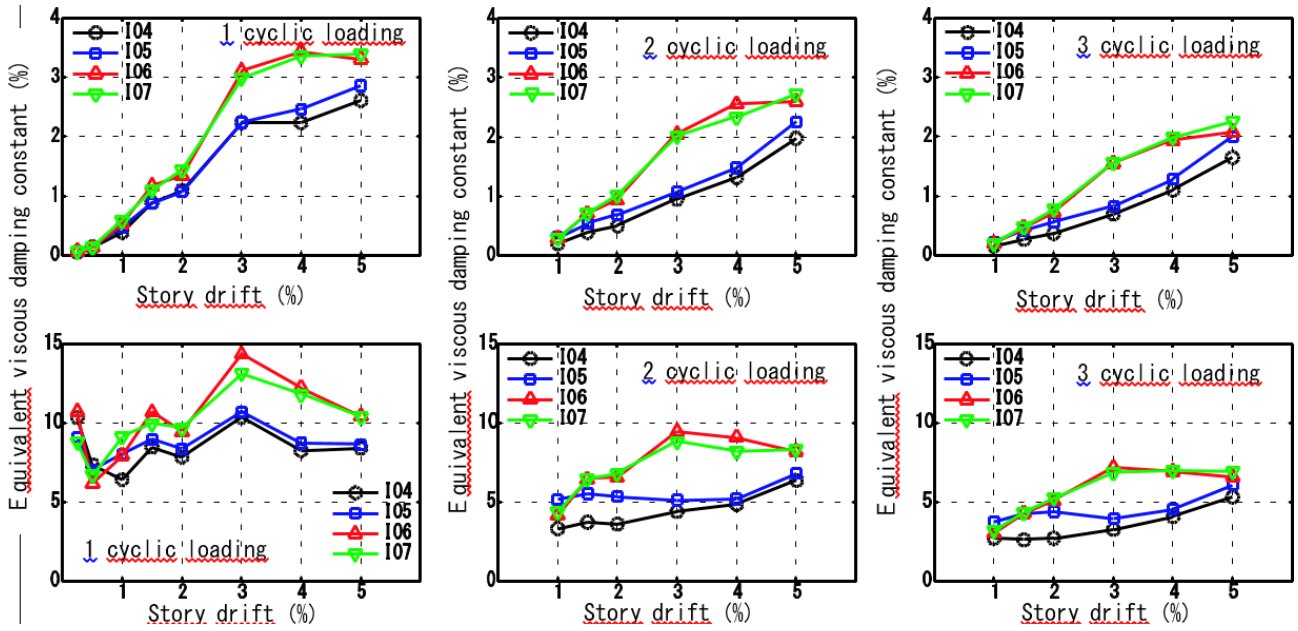

Figure 9. Hysteresis absorption energy - equivalent viscous damping constant.

When comparing the hysteresis absorbed energy of specimens I04 and I05, the hysteresis energy was almost the same until the first story ratio 3 % of loading. In the first loading of story drift ratio 4 % and in the subsequent second and third loading, the hysteresis absorbed energy of specimen I05 with a long-term shear force was 1.5 times to about 1.1 times greater than the hysteresis absorbed energy of specimen I04. Comparing the hysteresis absorbed energy of specimens I06 and I07, no significant differences were observed in the first, second, and third loading.

The equivalent viscous damping constant of specimens I04 and I05 was about 6 to 11 % in the first loading, about 3-7 % in the second loading, and about 3-6 % in the third loading. In a test of the long-term shear force for specimen I05, the equivalent viscous damping constant was a little larger than that of specimen I04. The equivalent viscous damping constant of specimens I06 and I07 was about 8 to 14 % in the first loading, about 4-10 % in the second loading and about 3-7 % in the third loading. In specimens I06 and I07 no significant difference was observed, and the equivalent viscous damping constant was not affected by the long-term shear force.

CONCLUSIONS

As a result of the undertaken static incremental positive and negative cyclic loading to test plane concrete beam-column joint portion of frames of 4 body sub-assemblages, the following findings are to be reported:

(1) Concerning the influence of the presence or absence of long-term shear force: the effect on the destruction situation and hysteresis properties of the test bodies is small. A reduced stiffness of the upper column posts is observed because the stress and deformation distribution of the frame changes. Further study on the seismic performance of frames is required in the future.

(2) In cases when a long-term shear force is applied to specimens with smaller column intensity ratio, yielding of top column posts main reinforcement occurred at an early stage and the deformation of the top posts increased. In specimens with larger column intensity ratio, such a trend was not observed.

(3) In specimens with small column intensity ratio, the maximal shear force was higher than the calculated value of the shear force at the time of beam ultimate bending by cross-sectional analysis, which does not take into account the strain hardening of the rebar; when taking into account the strain hardening of the rebar, it fell below the calculated value of the shear force during the beam ultimate bending.

(4) In the specimens with small column intensity ratio, when there is a long-term shear force (specimen I05), equivalent viscous damping constant at the time of the third loading is greater than in cases without long-term shear force (specimen I04) in the story drift ratio 1-3 %. In the specimens with large column intensity ratio, there is no difference in the equivalent viscous damping constant of the specimens due to the presence or absence of a long-term shear force.

ACKNOWLEDGEMENT

The first Author would like to express her special thanks to Prof. Hitoshi Shiohara for the opportunity of specializing at Tokyo University as well as to the programme AUSMIP+ for this chance and financial support, and to Assoc. Prof. Elena Dimitrova, the coordinator of the programme for Bulgaria, for advice and help.

REFERENCES

1. Shiohara, H., Kusuhara, F. (2014), *The next generation seismic design for reinforced concrete beam-column joints*, In: Proc. Tenth U.S. National Conf. on Earthquake Eng. (10NCEE), 2014, Anchorage, Alaska, USA, Earthquake Eng. Res. Inst. (EERI).
2. Kusuhara, F., Shiohara, H., Tazaki, W., Park, S.-Y. (2010), *Seismic performance of reinforced concrete interior beam-column joint under low ratio of column to beam moment capacity*, J Struct. Constr. Eng., AIJ, 75(656): 1873-1882. (in Japanese)
3. Kusuhara, F., Shiohara, H. (2012), *Joint shear? or column-to-beam strength ratio? Which is a key parameter for seismic design of RC beam-column joints, Test series on exterior joints*, In: Proc. 15th World Conf. on Earthquake Eng., Lisbon, Portugal, 2012.
4. AIJ Structural Committee, Design Guidelines for Earthquake Resistant Reinforced Concrete Buildings Based on Inelastic Displacement Concept, Architectural Institute of Japan, Tokyo, Japan, 1999. (in Japanese)
5. Park, R., Paulay, T., Reinforced Concrete Structures, John Wiley & Sons, Inc., 1975. doi: 10.1002/9780470172834
6. Kusuhara, F., Shiohara, H. (2006), *New instrumentation for damage and stress in reinforced concrete beam-column joint*, Proc. of 8th National Conf. on Earthquake Engineering, San Francisco, 2006, Paper No. 1214 on CD-ROM.